

RESEARCH ARTICLE

Mechanistic Analysis of Taxol-induced Multidrug Resistance in an Ovarian Cancer Cell Line

Ning-Ning Wang¹, Li-Jun Zhao¹, Li-Nan Wu¹, Ming-Feng He², Jun-Wei Qu¹, Yi-Bing Zhao¹, Wan-Zhou Zhao³, Jie-Shou Li⁴, Jin-Hua Wang^{1*}

Abstract

Objectives: To establish a taxol-resistant cell line of human ovarian carcinoma (A2780/Taxol) and investigate its biological features. **Methods:** The drug-resistant cell line (A2780/Taxol) was established by continuous stepwise selection with increasing concentrations of Taxol. Cell morphology was assessed by microscopy and growth curves were generated with in vitro and in vivo tumor xenograft models. With rhodamine123 (Rh123) assays, cell cycle distribution and the apoptotic rate were analyzed by flow cytometry (FCM). Drug resistance-related and signal associated proteins, including P-gp, MRPs, caveolin-1, PKC- α , Akt, ERK1/2, were detected by Western blotting. **Results:** A2780/Taxol cells were established with stable resistance to taxol. The drug resistance index (RI) was 430.7. Cross-resistance to other drugs was also shown, but there was no significant change to radioresistance. Compared with parental cells, A2780/Taxol cells were significantly heteromorphous, with a significant delay in population doubling time and reduced uptake of Rh123 ($p < 0.01$). In vivo, tumor take by A2780 cells was 80%, and tumor volume increased gradually. In contrast, with A2780/Taxol cells in xenograft models there was no tumor development. FCM analysis revealed that A2780/Taxol cells had a higher percentage of G0/G1 and lower S phase, but no changes of G2 phase and the apoptosis rate. Expression of P-gp, MRP1, MRP2, BCRP, LRP, caveolin-1, PKC- α , Phospho-ERK1/2 and Phospho-JNK protein was significantly up-regulated, while Akt and p38 MARK protein expression was not changed in A2780/Taxol cells. **Conclusion:** The A2780/Taxol cell line is an ideal model to investigate the mechanism of multi-drug resistance related to overexpression of drug-resistance associated proteins and activation of the PKC- α /ERK (JNK) signaling pathway.

Keywords: Ovarian carcinoma - Taxol - Multidrug resistance - signaling pathway

Asian Pac J Cancer Prev, 14 (9), 4983-4988

Introduction

Ovarian cancer is the second most common gynecological malignancy worldwide (Di Michele et al., 2009). At present, combination regimens containing taxanes (e.g. Taxol) are the most effective chemotherapy for ovarian cancer following optimal tumor debulking surgery (Di Michele et al., 2009). In some cases, the majority of patients initially respond well to the treatment, but they will inevitably suffer recurrence, largely due to drug or multidrug resistance (MDR). MDR is the ability of cancer cells to acquire resistance to various structurally and functionally different chemotherapeutic agents (Wu et al., 2003). MDR represents a major obstacle to the efficacy of chemotherapy. It is crucial to establish taxol-resistant ovarian cancer cell lines for understanding the mechanisms of MDR and enhancing the screening of chemotherapeutic drugs. However, there are few drug-resistant ovarian

cancer cell lines, especially taxol-resistant cells. In addition, the extant models also have some defect, such as lower resistant index, unclear biological features (Yan et al., 2007).

At present, the molecular mechanism of taxol resistance is not fully understood. Some common mechanisms include overexpression of some drug-resistant associated proteins including P-glycoprotein (P-gp) (Kim et al., 2013), protein kinase C- α (PKC- α) (Zhe et al., 2012), and activation of some signaling pathway including mitogen-activated protein kinase (MAPK) cascade and phosphatidylinositol-3-kinase (PI3K)/Akt signaling (Mackay et al., 2003; Hiss et al., 2012). Drug resistant mechanisms need further understand for solving some clinical problems.

In the study, the resistant cell line (A2780/Taxol) was induced by stepwise sequential exposure to increased concentration of taxol. Then the biological characteristics

¹Department of Gynecological Oncology Surgery, Jiangsu Cancer Hospital & Institute, Nanjing Medical University, ²Nanjing University of Technology School of Pharmaceutical Science, ³Sino-EU Biomedical Innovation Center (SEBIC), OG Pharma Corporation, ⁴Department of General Surgery, Nanjing General Hospital of Nanjing Military Command, PLA, Nanjing, Jiangsu, China *For correspondence: wangjinhua588@163.com

and underlying mechanisms were determined further. This cell line may serve as appropriate models for further study of mechanisms of taxol resistance in ovarian cancer.

Materials and Methods

Chemicals and reagents

Taxol was obtained from Taiji Pharmaceutical Co.Ltd (Sichuan, China). Cisplatin, 5-Fluorouracil (5-FU) and Rh123 were purchased from Sigma Chemical Co. (St Louis, MO, USA). Paclitaxel Liposome was from Iyvesike Pharmaceutical Co.Ltd (Jiangsu, China). Oxaliplatin and Docetaxel were from Hengrui Medicine Co.Ltd (Jiangsu, China). Doxorubicin Liposome, Nedaplatin was from aosaikang Pharmaceutical Co. (Jiangsu, China). Anti-P Glycoprotein antibody (ab3366) was from Abcam Biotechnology. Antibodies against β -actin, multidrug resistance-related protein1/2 (MRP1/2), breast cancer resistance protein(BCRP) or lung resistance-related protein (LRP), caveolin-1 and PKC α were obtained from Wuhan BOSTER Bio-engineering Co. (Hubei, China). Antibodies against Akt, Phospho-Akt at Ser473, p38 MAPK, Phospho-p38 MAPK (Thr180/Tyr182); p44/42 MAPK (Erk1/2), Phospho-p44/42 MAPK (Erk1/2) (Thr202/Tyr204), JNK, Phospho-JNK were from Cell Signaling Technology, Inc. (Beverly, Mass, USA). Bcl-2, Bax and horseradish peroxidase-linked (HRP) secondary antibody were from Nanjing Enogene Biotech Co.Ltd (Jiangsu, China). Cell apoptosis kit and cell cycle assay kit were from BIO-BOX Biotech Co.Ltd (Jiangsu, China). RIPA lysis buffer and bicinchoninic acid assay (BCA) kit were from Beyotime Institute of Biotechnology (Jiangsu, China).

Animal

Athymic nude mice (BALB/c-nu, female), 4 weeks old and weighing approximately 14 g, were purchased from Nanjing Model Animal Research Center (MARC). Animal certification label: SCXK2010-0001(china). All animals were provided sterilized food and water. All experiments were carried out in accordance with the guidelines on animal care and experiments of laboratory animals (Center of Experimental Animals, Nanjing University of technology, China), which was approved by the ethics committee for animal experiments.

Cell culture and Establishment of A2780/Taxol cell line

The human ovarian cancer cell line A2780 was obtained from Enogene Biotech Co. Ltd (Jiangsu, China). The A2780/Taxol cell line was intermittently exposure to doses of taxol at 100, 200, 400 and 800 ng/ml. The cells were incubated in taxol-containing medium for 48hs and were subjected again to taxol exposure when the cells entered logarithmic growth phase. This cyclic treatment was repeated four times over a period of six months. Finally, the taxolresistant cell line was generated and 800 ng/ml taxol was selected to maintain the drug-resistant phenotype. A2780 and A2780/taxol were cultured in RPMI1640 medium supplemented with 10% fetal bovine serum (FBS), 100 U/ml penicillin and 100U/ml streptomycin (GIBCOBRL, Paisley, UK) in a humidified

incubator containing 5% CO₂ at 37°C. Experiments were performed only after all the cells had been maintained in drug-free medium for two months.

Drug sensitivity assay

The cytotoxicities of Taxol, Docetaxel, Cisplatin, Oxaliplatin, Paclitaxel Liposome, and Doxorubicin Liposome were determined by MTT assay. Briefly, Monodispersed cells were collected with 0.25% trypsin-EDTA and resuspended to a final concentration of 1×10^5 cells/ml, and 100ul aliquots were seeded in 96-well plates. Following overnight preincubation, the medium was removed and replaced by various concentrations of the drugs mentioned above. Ten different concentrations for each drug were analyzed and three wells were used for each determination. Medium without drug was added to the control and blank wells. After 48h incubation, 15 ul of 5 mg/ml MTT solution was added to each well with the exception of the blank wells for 4 h at 37°C. After dissolving the resulting formazan product with dimethylsulfoxide (Sigma), absorbance value was measured at 490nm by enzyme linked immunosorbent assay. The IC₅₀ is defined as the dosage of drugs in which 50% of cellular death (50% reduction of absorbance at 490 nm) after 48h treatment. Resistant index (RI) = IC₅₀ of A2780/Taxol/IC₅₀ of A2780.

Analysis of morphological changes

Exponentially growing A2780 and A2780/Taxol cells were transferred to 60-mm dishes and allowed to adhere in 5% CO₂ at 37°C for at least 24 h. Then the cells were observed and photographed by a Nikon SMZ745T (Tokyo, Japan). In addition, cells (5×10^6) were collected, centrifuged, then small cell gobbets were fixed in 2.5% glutaraldehyde at 4°C for 2 h, postfixed in 1% osmic acid overnight at 4°C, and embedded in Epon812. Ultra-thin sections were made, stained and observed with an EM400T transmission electron microscope (Philips, Eindhoven, Netherlands).

Rhodamine123 accumulation

Briefly, 5×10^5 cells were incubated in 6-well plates and allowed to attach overnight. 5u mol/L Rh123 was added and the cells were incubated 2h in the dark at 37°C in 5% CO₂. Cells were then collected and washed twice with ice-cold phosphate-buffered saline (PBS) and resuspended in PBS with 10% FBS. The fluorescence intensity of intracellular Rh123 was recorded both by FACS scan flow cytometry (Becton Dickinson, San Jose, CA) and fluorescence microscope (OLYMPUS, Tokyo, Japan).

Cell cycle analysis

The A2780 and A2780/Taxol cells (5×10^5) were harvested and washed with PBS twice, centrifuged and resuspended with 0.3 ml of PBS, and fixed with ice-cold ethanol at 4°C overnight. The fixed cells were washed and resuspended in 1 ml PBS for 15min at room temperature, then incubated with 100ul RNase A at 37°C for 30 min followed by staining with 400ul propidine iodide (PI) for 30 min in the dark. Samples were analyzed for DNA content by FCM.

Cell apoptosis analysis by Annexin V/PI double staining

Annexin V/PI double staining and FCM were used to detect cell apoptosis. Cells (5×10^5) were seeded onto 6well plates. After 24h, cells were trypsinized, and diluted to 1×10^5 cells/ml, then centrifuged at 1500 rpm for 5 min. Cells were resuspended in 250ul binding buffer containing 2.5 ul of AnnexinV-EGFP and 20 ul of PI and mixed gently before fluorescence detection after 10 minutes. The fluorescence emitted by cells (10000 cells/sample) was analyzed using FCM.

Western blotting

The total cellular samples were harvested and rinsed twice with ice-cold PBS buffer. Cell extracts were collected in RIPA lysis buffer supplemented with 10 mM PMSF on ice for 30 min. Supernatants were collected after centrifugation at 12000 rpm for 15 min at 4°C. Protein concentration was determined using the BCA protein assay kit. 50-100ug of total protein were subjected to SDSPAGE gels and transferred onto polyvinyl difluoride membranes (Millipore, Bedford, MA) which were blocked with 5% skim milk (w/v) in tris-buffered saline containing 0.1% of Tween20 (TBST) at room temperature for 90min. Primary antibody incubation was performed at 4oC, overnight. Membranes were then washed by TBST and incubated with HRP-secondary antibody for 1h. Washing was repeated and bands were visualized by enhanced Chemiluminescence using the SuperSignal West Pico Chemiluminescent Substrate Kit (Pierce). Band intensities were analyzed by GelPro gel analysis software (BioRad). β -actin was used as the loading control for the experimental data analysis.

Nude mouse xenograft model.

The tumor-inoculated nude xenograft model was performed as previously described (LeBlanc et al., 2002; Chauhan et al., 2012). Twenty mice were randomized to two groups, each group was subcutaneously at the right armpit with 5.0×10^6 A2780 or A2780/Taxol cells in 200 μ l of PBS/matrigel (1:1) respectively. After tumor inoculation, tumor taken rate, growth speed and tumor size were examined for 4 weeks. The growth of primary tumors was monitored twice a week by measuring tumor diameters with calipers and calculating tumor volume using the formula: volume= $\text{width}^2 \times \text{length} / 2$.

Statistical analysis

All experiments were repeated at least three times. Data were analyzed by GraphPad Prism version 5.0 (GraphPad Software Inc., San Diego, CA) and SPSS 17.0 statistical software package (SPSS, IL, USA) and presented as mean \pm SD. Student's t-test was used and considered statistically significant at $p < 0.05$.

Results

Establishment and phenotype of the drug resistant cell line, A2780/Taxol cells. The Taxol-resistant A2780 (A2780/Taxol) cells were established over a period of six months and had stable resistance to Taxol in drug-free medium for at least two months before use. The resistance

Table 1. Drug sensitivity of A2780 and A2780/Taxol

Drug	n	IC50 (mean \pm SD, ug/ml)		
		A2780	A2780/taxol	RI
Taxol	3	0.01444 \pm 0.004168	4.92 \pm 0.3153*	340.7
Oxaliplatin	3	0.1373 \pm 0.04005	1.358 \pm 0.2103*	9.891
Paclitaxel Liposome	3	1.570 \pm 0.1452	263.5 \pm 2.598*	167.8
Doxorubici Liposome	3	2.061 \pm 0.1411	6.091 \pm 0.1282*	2.955
Nedaplatin	3	2.792 \pm 0.1340	5.520 \pm 0.1689*	1.977
Cisplatin	3	0.3607 \pm 0.02420	8.994 \pm 0.07809*	24.98
5-FU	3	4.476 \pm 0.2037	8.77 \pm 0.35*	1.9024

*Significant difference in comparison with the parental cells ($p < 0.01$). A2780 and A2780/taxol cells were exposed to indicated concentrations of above-mentioned drugs for 24 h and determined using the MTT assay. The IC50 values were calculated. Values of 3 independent experiments are represented as mean \pm SD

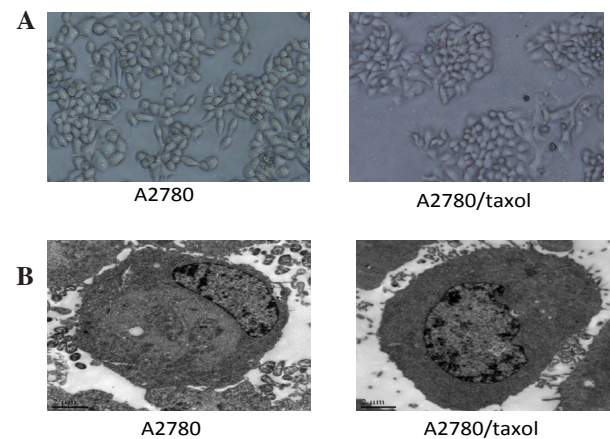


Figure 1. Morphology of A2780 and A2780/Taxol Cells in Exponential Phase. Morphological characteristics were determined using an inverted microscope at original magnification of x100 (A) and transmission electron microscope (B)

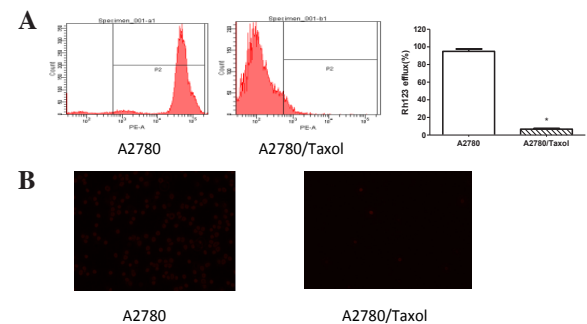


Figure 2. Rh123 Accumulation in A2780 and A2780/Taxol Cells. Rh123 (5 μ mol/L) was added, and the cells were incubated for 120 min. Rh123 fluorescence intensity of each sample was measured using flow cytometry (A). Rh123 accumulation was also detected using fluorescence microscope (B). Columns, means of triplicate determinations; bars, SD; * $P < 0.001$, versus the parent control group

index of Taxol in A2780/Taxol cells was 340.7 by MTT assay. The drug sensitivity data of A2780 and A2780/Taxol cells to other chemotherapeutic drugs are shown in Table 1 and Figure 1. The results indicated that the A2780/Taxol cells displayed cross-resistance to these drugs.

Cellular morphology and growth rate. Using an inverted phase-contrast microscope, A2780 cells had a relatively uniform cell size and shape, while A2780/Taxol grew in clusters, and varied in size and shape (Figure 2A).

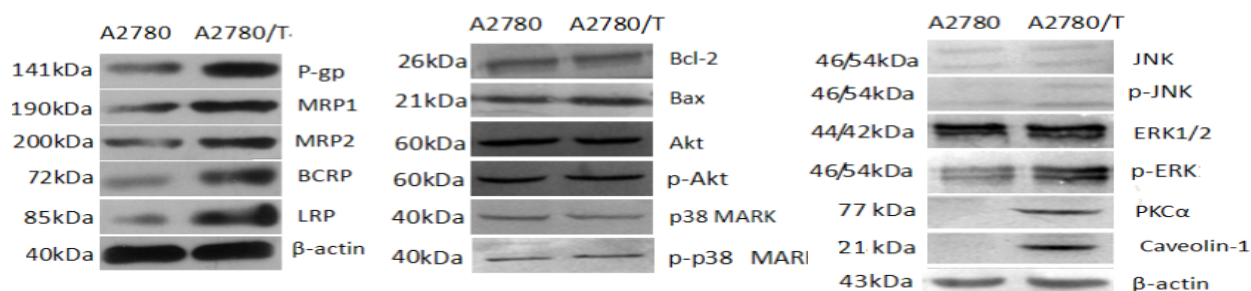


Figure 3. Analysis of the Drug-resistant Related Signaling Pathway in A2780/Taxol Cells. Total cell lysates from both A2780 and A2780/Taxol cells were subjected to immunoblot analysis with antibody specific. Protein expression levels after normalized relatively to that of β-actin. All immunoblot analyses performed in the current study are representatives of at least three independent experiments

Table 2. Cell Cycle Distribution of A2780 and A2780/Taxol Cells

Cell lines	Percentage of each cell cycle		
	G0/G1	S	G2/M
A2780	46.41±0.7783	36.71±0.8556	16.88±1.564
A2780/Taxol	62.8±1.079*	21.63±0.8570*	15.57±0.6888

**P* < 0.001, vs A2780 cells

Using transmission electron microscope (TEM), A2780/Taxol had an increased ratio of nuclei to cytoplasm, irregular nuclear membrane and obvious cell protrusions (Figure 2B). The growth rate of A2780/Taxol (24.22 h ± 0.22) was significantly (*p* < 0.01) slower than parental cells (20.60 h ± 0.35) (Figure 3).

Rh123 accumulation. To ascertain the potential mechanism of Taxol resistance in A2780/Taxol cells, we examined fluorescence intensity (%) of intracellular Rh123 in A2780 (94.90±1.595) and A2780/Taxol (6.733±0.4096) cells (Figure 4A, *p* < 0.001). When cell density in both cells at the same level, the accumulation of intracellular Rh123 was determined by fluorescence microscopy and Rh123 accumulation was found to be significantly decreased in MDR cells (Figures 4B). Taken together, these results indicated that over-expression and/or function-improving of some drug efflux transporters in A2780/Taxol cells results in the expulsion of chemotherapeutic drugs, thereby leading to drug resistance.

Cell cycle distribution and apoptosis analysis. Cell cycle distribution are shown in Table 2. There was a significant decrease observed in the percentage of taxol resistant cells in S phase compared to parental cells with a corresponding increase in G0/G1 phase (*p* < 0.001). There was no significant difference between the two cells in G2/M phase or apoptosis.

Expression of drug resistance-related proteins. Expression of drug resistance-related proteins were evaluated in the Taxol resistant cells and compared to their parental cells to identify possible changes in these proteins that may occur following Taxol resistance. Western blot analysis confirmed that the P-gp, MRP1, MRP2, BCRP, LRP, PKC-α, caveolin-1, Phospho-ERK1/2, Phospho-JNK proteins in the A2780/Taxol were all significantly increased (*p* < 0.01). Whereas, no significant changes in Bcl-2, Bax, Akt and Phospho-Akt, ERK1/2, JNK, p38 MARK and Phospho-p38 MARK expressions were noted between the two cell lines.

Tumorigenicity of A2780 or A2780/Taxol cells in nude

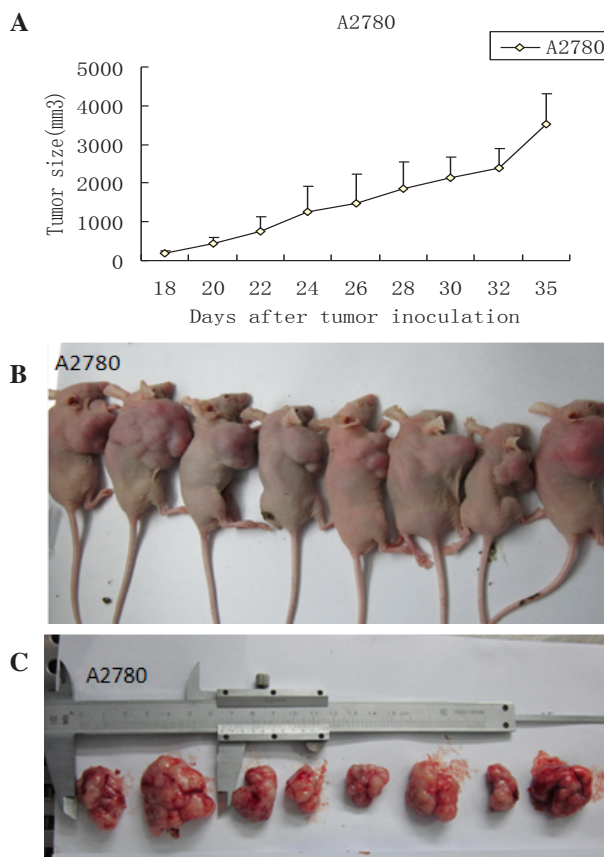


Figure 4. Tumorigenicity of A2780 Xenograft Model in Athymic Nude Mice. A. Tumor growth curve with time after cell inoculation. Points, mean tumor size for eight mice after implantation; bars, SD. B, tumors in the right armpit of female nude mice on the 32th day after implantation. Eight of ten mice have tumor take. C, tumor size. Tumors were removed on the 32th day after inoculation

mouse xenograft model. A2780 cells implanted into the right armpit of female nude mice rapidly form tumors at the site of injection. Tumor take by A2780 cells is 80% (eight of ten mice), and tumor volume was increased gradually. In contrast, A2780/Taxol cells xenograft models were no tumor development (the tumor take was 0%) (Pictures were not shown).

Discussion

In the study, we successfully established a taxol resistant cell line, A2780/Taxol, by incremental Taxol-exposure for six months. After 2 months of culture in taxol-free medium, A2780/Taxol cells also kept the

same resistance to Taxol. Compared with the parental cells, the resistance index was 340.7. To some extent, it also showed different cross-resistance to some common chemotherapeutic drugs such as Paclitaxel Liposome, Cisplatin, Oxaliplatin in different structures and mechanisms, but no significant change to radioresistance (data were not shown). The biological features of the drug-resistance cells were found in our data. The resistant subline grew slower, and the population doubling time was extended as compared with parental cells A2780. This might be caused by the existence of non-cycling dormant cells (Wen et al., 2009). Having shown that growth inhibition in A2780/Taxol cells in vitro, we next examined it in vivo using tumor xenograft mouse model. We found that drug-resistant ovarian cancer-bearing mice were no tumor development, In contrast, the parental cells-bearing mice have 80% tumor take, and tumor size was increased gradually. These in vivo data confirm our in vitro findings. Moreover, cell cycle analysis showed that the percentage of G0/G1 in A2780/Taxol cells was higher than in A2780. But the percentage of S phase was lower than that of A2780 cells in corresponding phases. There is a critical balance between cell cycle arrest and cell death following chemotherapy.

There were some morphologic changes in A2780/Taxol cells. The cells were more heteromorphous than A2780 in size and shape. It grew in clusters, and most of them exhibited a fibroblastic shape. TEM revealed that there were some sharp needle-like protrusions from cell membrane. These were similar to changes of epithelial-mesenchymal transition (EMT). EMT is a biological and molecular process in which epithelial cells lose cell polarity and gain a fibroblastic spindle-shape morphology allowing them to infiltrate tissues and invade organs, which was regarded as one of the reasons leading to drug resistance (Paraiso et al., 2013). Then caveolin-1, which is the main constituent molecule of caveolae at cell membrane, acts as a crucial modulator of EMT (Salem et al., 2011). In this study, we noticed that caveolin-1 was overexpressed in A2780/Taxol cells. These data might indicate that caveolin-1 expression profoundly alter cellular morphology via induction of EMT, which is associated with taxol resistance in ovarian cancer.

The mechanism of MDR is complicated (Szakács et al., 2006; Sui et al., 2012), and involves multiple mechanisms including increased drug efflux, altered anti-cancer drug targets, reduced drug activation, enhanced DNA damage repair capacity. Among them, increasing drug efflux was the most common phenomenon of weakening the effects of cytotoxic drugs. The methods of increasing drug expulsion include improving the activity of drug efflux transporters or increasing these expression levels. Transporter proteins include ATP-binding cassette (ABC) transporter superfamily, such as P-gp, MRP1, MRP2, and BCRP. Also, LRP could confer drug resistance by redistributing drugs away from intracellular targets (Pérez-Tomás, 2006). Therefore, we used Rh123 assay and Western blotting to detect the function and the expression of these transporters in A2780 and A2780/Taxol cells. Our results showed that intracellular Rh123 concentration and some transporters were all significantly increased in A2780/Taxol cells. The

over-expression of some transporters in A2780/Taxol cells results in the expulsion or redistribution of anti-tumor drugs in cells and may play a role in drug resistance.

Other mechanisms of drug resistance involve in alteration the apoptotic response. The apoptotic family includes death antagonists such as Bcl-2 and death agonists such as Bax (Liu et al., 2011). Our data showed the Bcl and Bax levels and the percentage of cell apoptosis were not significantly altered in both cells, the drug resistance seen in the A2780/Taxol cells is not dependent on the Bcl-2 and Bax-dependent apoptotic mechanism. In addition, cellular responses toward cytotoxic drugs are also modulated by crosstalk between oncogenic signaling cascades and resistance mechanisms. Recently, growing evidence suggests activation of PKC- α (Zhao et al., 2012), MAPK cascade and PI3K/Akt signaling (Hiss, 2012) play important roles in chemo-resistance of ovarian cancer. The MAPK family has been classified into 3 distinct subfamilies: the extracellular signal-regulated protein kinases (ERKs) including ERK1/2, the stress-activated c-Jun N-terminal protein kinase (JNKs) and p38 kinase (Hoshino et al., 1999; Doddareddy et al., 2012). The MAP kinase cascade and PI3K/Akt are all effectors of Ras signaling (Downward, 2003; McCubrey et al., 2012), which have been implicated in a wide range of cellular functions, including proliferation, survival, migration, malignant transformation (Wee et al., 2008; Yang et al., 2013), and also in the development of drug resistance (Navolanic et al., 2003; Sui et al., 2012). In our study, we found that JNK and ERK1/2 were activated in A2780/Taxol cells. However, neither were these differences between parental and taxol resistant cells in Akt or p38 MARK protein expression. It might suggest that activation of Akt and P38 MARK was not involved in the MDR in A2780/Taxol cells, and the increased activities of the JNK and ERK1/2 signaling pathway were associated with resistance to chemotherapy. PKC- α were overexpressed in A2780/Taxol cells, which was consistent with our previous findings in other drug resistant cells (Wang et al., 2010), which indicates that PKC- α plays very important roles in MDR. Then PKC- α was preferentially responsible for triggering MARK signaling pathway (Tanaka et al., 2003). Our data showed similar to the results. So these activations must be directly or indirectly related to an as yet unknown oncogenic event.

In summary, we established the stable taxol resistant cell line of ovarian cancer, A2780/Taxol successfully. It also showed cross-resistance to many different chemotherapeutic drugs in different structures and mechanisms. This indicated that A2780/Taxol was a wonderful cell model for MDR research. According to our findings, the overexpression of caveolin-1 might alter cell membrane morphology via induction of EMT, which can be associated with MDR. Moreover, we speculated that some of MDR did not rely on Bcl-2/Bax-dependent apoptotic response, and some signal pathways, including PI3K/Akt and p38 MARK cascades. The multidrug resistance-related proteins and the activation of PKC- α /ERK (JNK) signaling pathways may play important roles on MDR. These changes may be linked to each other, but further research is needed.

Acknowledgements

This work was supported by grants from Jiangsu Government Six Major Talent Fund (2008-D-02), Jiangsu Administration of Traditional Chinese Medicine (LZ09082), Jiangsu Government Scholarship “333” Plan and Jiangsu Key Medical Personnel (RC2011091). The author(s) declare that they have no competing interests.

References

- Cantley LC (2002). The phosphoinositide 3-kinase pathway. *Science*, **296**, 1655-7.
- Chauhan D, Tian Z, Nicholson B, et al (2012). A small molecule inhibitor of ubiquitin-specific protease-7 induces apoptosis in multiple myeloma cells and overcomes bortezomib resistance. *Cancer Cell*, **22**, 345-58.
- Di Michele M, Della Corte A, Cicchillitti L, et al (2009). A proteomic approach to paclitaxel chemoresistance in ovarian cancer cell lines. *Biochim Biophys Acta*, **1794**, 225-36.
- Doddareddy MR, Rawling T, Ammit AJ (2012). Targeting mitogen-activated protein kinase phosphatase-1 (MKP-1): structure-based design of MKP-1 inhibitors and upregulators. *Curr Med Chem*, **19**, 163-73.
- Downward J (2003). Targeting RAS signaling pathways in cancer therapy. *Nat Rev Cancer*, **3**, 11-22.
- Hiss D (2012). Optimizing molecular-targeted therapies in ovarian cancer: the renewed surge of interest in ovarian cancer biomarkers and cell signaling pathways. *J Oncol*, **2012**, 737981.
- Hoshino R, Chatani Y, Yamori T, et al (1999). Constitutive activation of the 41/43-kDa mitogen-activated protein kinase signaling pathway in human tumors. *Oncogene*, **18**, 813-22.
- Kim H, Park GS, Lee JE, et al (2013). A leukotriene B4 receptor-2 is associated with paclitaxel resistance in MCF-7/DOX breast cancer cells. *Br J Cancer*, **109**, 351-9.
- LeBlanc R, Catley LP, Hideshima T, et al (2002). Proteasome inhibitor PS-341 inhibits human myeloma cell growth in vivo and prolongs survival in a murine model. *Cancer Res*, **62**, 4996-5000.
- Liu HZ, Yu C, Yang Z, et al (2011). Tubeimoside I sensitizes cisplatin in cisplatin-resistant human ovarian cancer cells (A2780/DDP) through down-regulation of ERK and up-regulation of p38 signaling pathways. *Mol Med Report*, **4**, 985-92.
- Mackay HJ, Twelves CJ (2003). Protein kinase C: a target for anticancer drugs? *Endocr Relat Cancer*, **10**, 389-96.
- McCubrey JA, Steelman LS, Chappell WH, et al (2012). Ras/Raf/MEK/ERK and PI3K/PTEN/Akt/mTOR cascade inhibitors: how mutations can result in therapy resistance and how to overcome resistance. *Oncotarget*, **3**, 1068-111.
- Navolanic PM, Steelman LS, McCubrey JA (2003). EGFR family signaling and its association with breast cancer development and resistance to chemotherapy (Review). *Int J Oncol*, **22**, 237-52.
- Paraiso KH, Smalley KS (2013). Fibroblast-mediated drug resistance in cancer. *Biochem Pharmacol*, **85**, 1033-41.
- Pérez-Tomás R (2006). Multidrug resistance: retrospect and prospects in anti-cancer drug treatment. *Curr Med Chem*, **13**, 1859-76.
- Salem AF, Bonuccelli G, Bevilacqua G, et al (2011). Caveolin-1 promotes pancreatic cancer cell differentiation and restores membranous E-cadherin via suppression of the epithelial-mesenchymal transition. *Cell Cycle*, **10**, 3692-700.
- Sui H, Fan ZZ, Li Q (2012). Signal transduction pathways and transcriptional mechanisms of ABCB1/Pgp-mediated multiple drug resistance in human cancer cells. *J Int Med*

Res, **40**, 426-35.

Szakács G, Paterson J, Ludwig JA, et al (2006). Targeting multidrug resistance in cancer. *Nat Rev Drug Discov*, **5**, 219-34.

Tanaka Y, Gavrielides MV, Mitsuchi Y, et al (2003). Protein kinase C promotes apoptosis in LNCaP prostate cancer cells through activation of p38 MAPK and inhibition of the Akt survival pathway. *J Biol Chem*, **278**, 33753-62.

Wang JH, Zhao WZ, Chen XX, et al (2010). Establishment and biological characterization of Cisplatin-resistant cell line OV1228/Taxol of ovarian carcinoma. *Chin J Cancer Prev Treat*, **22**, 281-4.

Wee S, Wiederschain D, Maira SM, et al (2008). PTEN-deficient cancers depend on PIK3CB. *Proc Natl Acad Sci U S A*, **105**, 13057-62.

Wen J, Zheng B, Hu Y, et al (2009). Establishment and biological analysis of the EC109/CDDP multidrug-resistant esophageal squamous cell carcinoma cell line. *Oncol Rep*, **22**, 65-71.

Wu DL, Huang F, Lu HZ (2003). Drug-resistant proteins in breast cancer: recent progress in multidrug resistance [J]. *Chin J Cancer*, **22**, 441-4. [in Chinese]

Yan XD, Li M, Yuan Y, et al (2007). Biological comparison of ovarian cancer resistant cell lines to cisplatin and Taxol by two different administrations. *Oncol Rep*, **17**, 1163-9.

Yang SH, Sharrocks AD, Whitmarsh AJ (2013). MAP kinase signalling cascades and transcriptional regulation. *Gene*, **513**, 1-13.

Zhao LJ, Xu H, Qu JW (2012). Modulation of drug resistance in ovarian cancer cells by inhibition of protein kinase C-alpha (PKC- α) with small interference RNA (siRNA) agents. *Asian Pac J Cancer Prev*, **13**, 3631-6.

Zhe C, Li-Juan W, Ming Hui W, et al (2011). Mechanism governing reversal of multidrug resistance in human breast carcinoma cells by chelerythrine. *Zhongguo Yi Xue Ke Xue Yuan Xue Bao*, **33**, 45-50.